NEW FEA SHELL ELEMENT MODEL FOR SEAM WELD STATIC AND FATIGUE STRUCTURAL ASSESSMENT

Didier Turlier[a], Patrice Klein[a], Laurent De Noni[a], Didier Lawrjaniec[b]

[a] LOHR Industrie, Hangenbieten, France. virtual.testing@lohr.fr
[b] Institut de Soudure, Yutz, France. d.lawrjaniec@institutdesoudure.com.

Abstract. The innovative approach consists of a new weld seam representation using an inclined shell element for the weld joint structural analysis. The shell seam mesh is connected to the sheet solids using FEA glue connectors which do not provide any additional rigidity in the assembly. This special weld element enables to assess the weld throat strength for static load or fatigue load. For static, equivalent stress according to Eurocode 3, or other standard, may be displayed at each weld element along the seam length. For fatigue, the structural stress approach uses linearized stress distribution over the throat thickness, which is well suited to the shell element use. This method has been verified first by calculating the resulting loads throughout the throat thickness, then by comparing the stiffness of the assembly obtained from either a fine solid fem model or a coarse shell model. The approach is validated. It correlates test results when the fatigue crack initiation direction is in the weld leg section. Extensive testing is performed in collaboration with Institut de Soudure. Samples are based on asymmetric fillet weld T assemblies with several plates and weld throat thickness, different penetration depths and with two types of loading which lead to the bending of the weld. Root cracks occur either though the throat, but not in the weld leg section, or through the base plate thickness. In those cases, the established structural stress criterion is not appropriate and two improvements are proposed. First, when weld leg sizes are unbalanced or when shear stress in the leg section is high, the structural stress is evaluated by scanning all the throat sections in order to reach the maximum normal stress value. Secondly, when both the weld and the flange plate are subject to bending, the root crack may propagate through the flange plate. The stress distribution is biaxial and the two normal stresses are combined. The resultant stress gives conservative result. LOHR uses NX from SIEMENS PLM Software as CAD and CAE pre/post solutions. Automation toolboxes have been developed that help the model preparation process based on a CAD solid representation of the weld. The programs create the weld toe contour and the weld element to sheet metal element connections. The automation is a necessity in order to avoid the tedious manual meshing process. The CAD associative feature helps for iterative analyses because the FEA model is updated when the design is changed. The industrial application of the method is demonstrated by a complete car carrier trailer structural analysis. FEA post processing tools have been developed to allow a global structure display with seam weld specific results.

1 INTRODUCTION

As a manufacturer of large welded-structure vehicles, LOHR aims at optimizing process cost. Seam welding, mainly fillet welds, is an important part of the manufacturing process. Fewer seams, throat size reduction, and intermittent welds are solutions for cost-effectiveness. The strength of the assembly remains to be ensured. In FEA, weld modeling becomes crucial for such detailed needs. For large sheet metal structure analysis the use of shell element is appropriate. LOHR Industrie's "seam sim" project objective is to combine those two requirements and it leads to the elaboration of an innovative model where weld joints are represented by shell elements for structural stress calculation. Extensive testing will be needed in order to prove the efficiency of the model. Improvements of the structural stress criterion might be useful in order to fit all types of root cracking paths. Automation of the CAD/CAE process from the *Seam* solid to the *Sim*ulation is also part of the project in order to avoid tedious manual meshing. Finally dedicated post-processing tools will be developed in order to have an efficient solution for the weld result display within a large structure model.

2 FEA SEAM WELD MODEL

The proposed FEA model of the seam weld has been already presented in FEA or welding events or publications [1,2]. It is illustrated on figure 1. It uses a shell element which connects two node contours. The nodes fit with the mid-width lines of the two weld leg sections. The connection of the weld leg lines to the metal plate is performed with the FEA gluing technique with no additional rigidity. As shown in figure 1, it uses both a rigid 1D element (RBE) connection from the weld leg node (point A) to a projected node on the metal plate (point B) and a multi point constraint (MPC) connected from point B to the element of the metal plate.

For 3D complex assembly, the load distribution depends on the components stiffness. In order to obtain the right load flux, the weld model stiffness has to be equivalent to the real stiffness of the seam weld joint. As illustrated in figure 2, by assigning the weld throat size as thickness of the weld shell element, it has the same section area as the physical weld and similar transverse and longitudinal stiffness. In figure 2, the blue section represents the shell

element area and the red section the physical weld area. The technique is also convenient for overlap joint or corner joint modelling as shown in figure 3. Weld shell element may be connected to solid element by using this technique in case of thick part welded assembly.

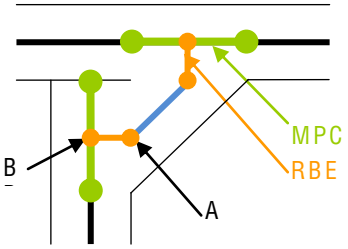

Figure 1: Shell element connection

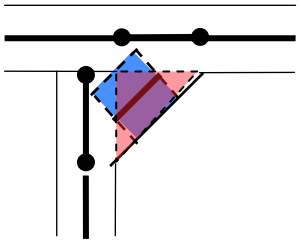

Figure 2: Element thickness

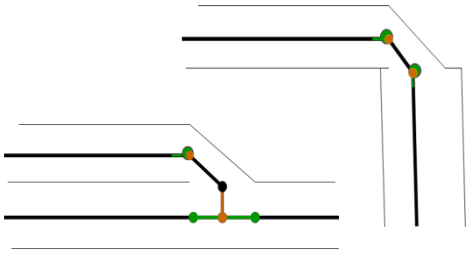

Figure 3: Other types of weld

3 STRESS CALCULATION

For static strength assessment, the equivalent stress is calculated at the centre of the weld shell element by using Eurocode3 formulas [4] and the resulting value is compared to the base material ultimate strength.

$$\sigma_{eq} = \sqrt{\sigma_{\perp}^{2} + 3 \times (\tau_{\perp}^{2} + \tau_{II}^{2})}$$

With the stress components shown in figure 4:

σ_{eq} : Equivalent stress,

$\sigma_{\perp}$: Normal stress orthogonal to weld throat,

$\tau_{\perp}$: Shear stress orthogonal to weld line,

$\tau_{//}$: Shear stress parallel to weld line

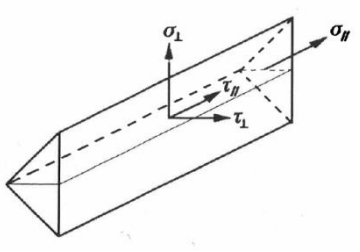

Figure 4: Weld stresses

For fatigue assessment, analyses are based on the structural stress calculation. It may be performed based on the normal stress at the weld toe or at the weld root locations. The structural stress calculation, as mentioned by Niemi et al in [4], may be calculated by linearization of the stress distribution through the base plate thickness at the weld toe. The structural stress is the combination of the membrane normal stress and the bending normal stress. The method has been extended to the weld leg section in the continuation of the root face by Fricke for weld root fatigue assessment when the weld throat is subjected to bending [5] This approach is based on the linearization of the normal stress $\sigma_x(z)$ within the weld leg section, see figure 5. The two components of normal stress are evaluated using the following formulas:

$$\sigma_{m,w} = \frac{1}{b.\lambda} \cdot \sum P_{xi}$$

$$\sigma_{b,w} = \frac{6}{b.\lambda^{2}} \cdot \sum \left(P_{xi} \cdot \left(\frac{\lambda}{2} - z \right) \right)$$

$$\sigma_{S,w} = \sigma_{m,w} + \sigma_{b,w}$$

With: $\sigma_{m,w}$: membrane stress
$\sigma_{b,w}$: bending stress
$\sigma_{s,w}$: structural stress
b: weld length
λ: leg length
P_{xi}: normal force

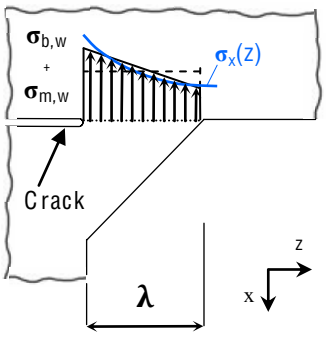

Figure 5: Weld leg stress distribution

The method is applicable when the shear stress in the section is less than 20% of the normal stress, when it is higher the principal stress orientation and the crack path change. In FEA, the structural stress is calculated from the nodal forces in the weld leg section by using solid element meshing. This has been extended to shell element model in [6] by using the appropriate element node location at the mid-line of the weld leg section, see figure 6. The two stress components may be computed from the internal forces f_w and moments m_w per unit of length. They are obtained by transformation of nodal forces using the shell element shape functions.For steel structure and at the weld toe, the associated fatigue classes are FAT 90 - FAT 100, which are the fatigue strength S-N curves at 2 millions cycles for a survival probability of 97.7%, as given in chapter 3.3 of the IIW recommendations [7].

$$\sigma_{m,w} = \frac{f_w}{\lambda}$$

$$\sigma_{b,w} = \frac{6.m_w}{\lambda^2}$$

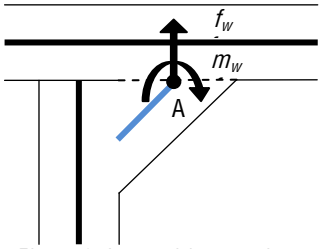

Figure 6: Internal force and moment

The effect of the thickness may be taken into account when plate thickness t exceeds 25 mm. The reduction factor is $(25/t)^n$, with n depending on weld type, n=0.3, in case of as-welded T-joint [7]. At the weld root, FAT80 has been found appropriate by Fricke [5]. Mean stress effect may modify the fatigue strength and several methods to determine its influence factor are given in [7,8,9]. For weld root fatigue assessment in steel structure, the Sonsino approach [9] is used and the correction factor is illustrated in figure 7.

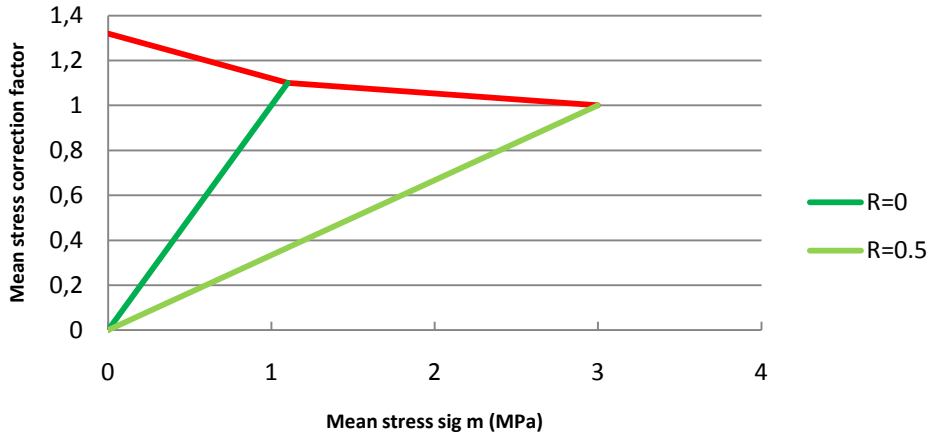

Figure 7: Mean stress infuence factor

In case of multi-axial stresses, interaction formula can be used describing the combined effect of two or more stress components. In Sonsino publication [10], σ_{res} and $\tau_{\parallel}$ are used and compared with reference stresses. This approach is based on the Gough-Pollard algorithm. It considers a multi-axial parameter which equals one when the structure is made of steel and the multi-axial stress components are proportional. The criterion shall be complied but the approach does not allow damage calculation.

$$\left(\frac{\sigma_{res}}{FAT(\sigma)}\right)^2 + \left(\frac{\tau_{\parallel}}{FAT(\tau)}\right)^2 \leq 1$$

The structural stress is used as σ_{res} and the torsional shear stress is $\tau_{\parallel}$. The FAT(σ) is depending on the weld area, FAT90 - FAT100 at the weld toe and FAT80 at the weld root. For shear stress FAT(τ) =FAT80, based on recommendations [7].

4 VERIFICATION AND VALIDATION

4.1 Verification

The shell element model results are verified by comparing to fine modeling results. Both rigidity and stress evaluation are verified. The following steel assembly, illustrated in figure 8, is analyzed using 2D plane stress theory. Element size is around 0.25 mm in the weld area. The shell element method analysis is performed with element size around 10 mm, see Figure 9. Both transverse and axial loads applied at the top of the upper web are investigated.

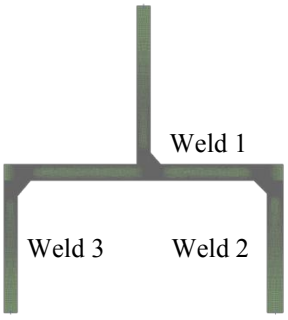

Figure 8: 2D plane stress model

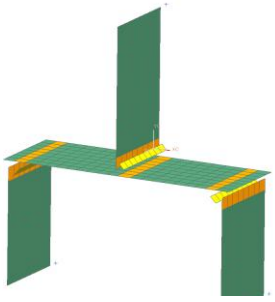

Figure 9: Shell element model

Table 1: Structural stress (MPa)

		2D plane stress			Shell element model			
	Weld Id	σm,w	σb,w	σs,w	σm,w	σb,w	σs,w	% error σs,w
Axial load	1	1,11	-3,89	5,00	1,11	-3,89	5,00	0,00
load	2	-0,69	-5,14	4,45	-0,70	-5,38	4,68	4,46
1000 N	3	-0,64	-3,01	2,37	-0,64	-3,08	2,45	2,43
Transverse	1	0,00	-66,67	66,67	0,00	-66,67	66,67	0,00
load	2	1,17	17,26	-16,08	1,18	17,50	-16,32	1,39
1000 N	3	-1,17	-2,56	1,38	-1,18	-2,42	1,24	5,43

Structural stresses are evaluated and table 1 gives the results for the two approaches. The error is zero when considering the specimen joint of the upper web on which the load is applied, because the two methods give the load resultant calculation at the same geometric point. The equivalence is due to static load equilibrium theory. Errors occur at the lower web joints, for which the load distribution determination depends on the joints and plates stiffness. The maximum error is 5 % which is a little discrepancy considering the large mesh size reduction. The appropriate stiffness of the weld joint idealization is a key parameter. When comparing the maximum deflection, which is located at the load application point, the larger error is obtained in the case of transverse load and the coarse shell model is 4.2% stiffer than the fine model. Considering the specimen width as large, the computation is performed using a plane strain theory. Then, displacement error increases, the coarse shell model is 6% softer.

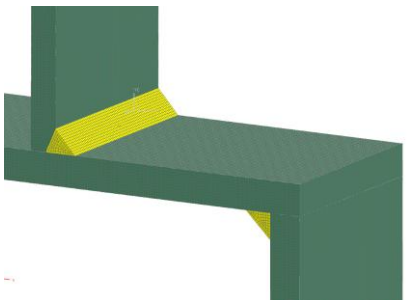

Figure 9: Fine 3D volumic element model

Table 2: Maximum deflection magnitude (mm)

	2D plane stress	2D plane strain	3D Solid	3D Shell	3D shell	max 3D
load 1000 N	Quad 4	Quad 4	Hexa 8	Quad 4	Quad 8	% error
Axial	7,48E-02	6,80E-02	7,12E-02	7,14E-02	7,15E-02	0,40
Transverse	6,83E-01	6,21E-01	6,42E-01	6,54E-01	6,60E-01	2,83

Using 2nd order element for the coarse shell model, the results are similar. In order to finalize the stiffness assessment, results are compared to a fine 3D solid element calculation. See model in figure 9. The maximum deflection error between the coarse shell model and the refined 3D model reaches only 2.8%. The proposed shell element approach gives a very good correlation with the 3D fine solid element model considering the element number reduction factor which is about one thousand.

4.2 Validation

Validation is performed with two kinds of physical tests: a tensile load specimen and the bending of a tube [11,12]. A tensile load test, with 7 specimens made of 6 mm thick steel plates and fillet welds with a throat size a=5 mm, see figure 10. The fatigue load ratio is R=0.5. The crack propagates in the weld leg section, see figure 11.

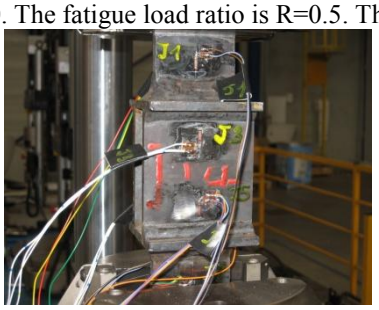

Figure 10: Tensile test

Figure 11: Crack along the weld leg section

Calculation of the structural stress is performed by considering the distortion of each specimen. The misalignment of the two clamped webs induces asymmetric behaviour which is introduced in the FEA model. Structural stress results are given in the table 3.

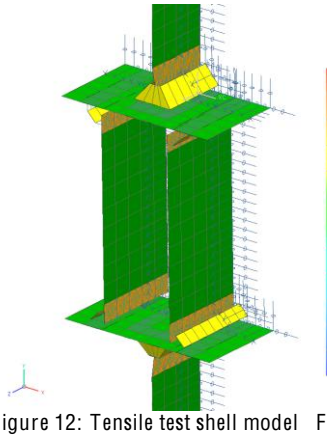

Figure 12: Tensile test shell model

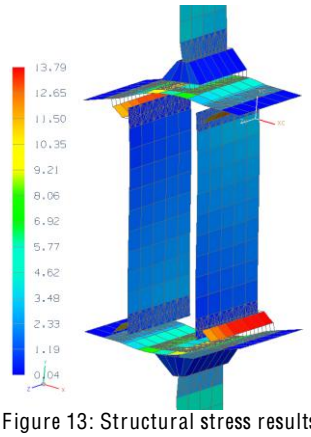

Figure 13: Structural stress results (MPa)

Table 3: Tensile test model structural stress ranges in the leg section

	A1	A2	A3	A4	A5	A6	A7
nbr of cycles N	1204769	1541470	1092468	1390000	1900762	1787853	1437126
$\Delta\sigma$, R=0.5 (MPa)	132	134	143	154	155	144	156

The bending tests are performed using 200x100x10 rectangular members welded on a 60 mm thick plate. Bending load is applied with a R=0.1 load factor. Five specimens are tested with three different weld preparation configurations as described in figure. 14.

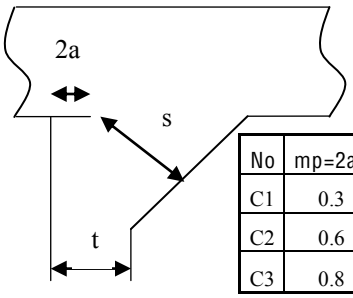

No	mp=2a/t	t (mm)	s (mm)
C1	0.3	10	10.6
C2	0.6	10	6
C3	0.8	10	6

Figure 14: Weld configurations

Figure 15: Bending test

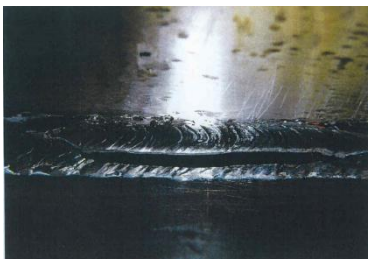

Figure 16: Crack through the weld

Structural stress is computed using shell mesh model and results are given in the following table. To convert the structural stress from load ratio R=0.1 to R=0.5, the mean stress influence factor is 1.09.

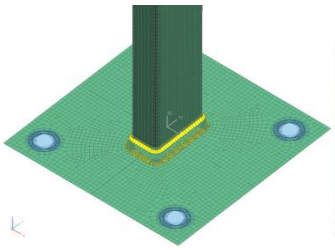

Figure 17: Bending test model

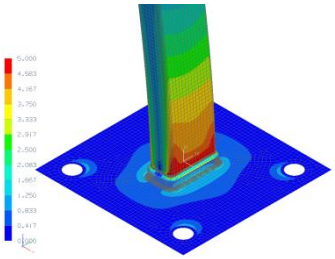

Figure 18: Stress results (MPa)

Table 4: Bending test model, maximum structural stress ranges $\Delta\sigma_s$ in the leg section

	C1-1	C1-2	C2-3	C3-4	C3-5
nbr of cycles N	>2000000	340000	160000	>2000000	1200000
$\Delta\sigma_s$ R=0.1 (MPa)	102	206	353	126	195
$\Delta\sigma_s$ R=0.5 (MPa)	94	190	325	116	180

All the results are compiled in figure 19. Results computed thanks to the proposed shell element approach show a good agreement with Fricke results FAT 136, see [5]. FAT80 may be used as a safety design criterion. The method allows the fatigue assessment as regards as root cracking for fillet weld subject to throat bending when crack occurs in the weld leg section.

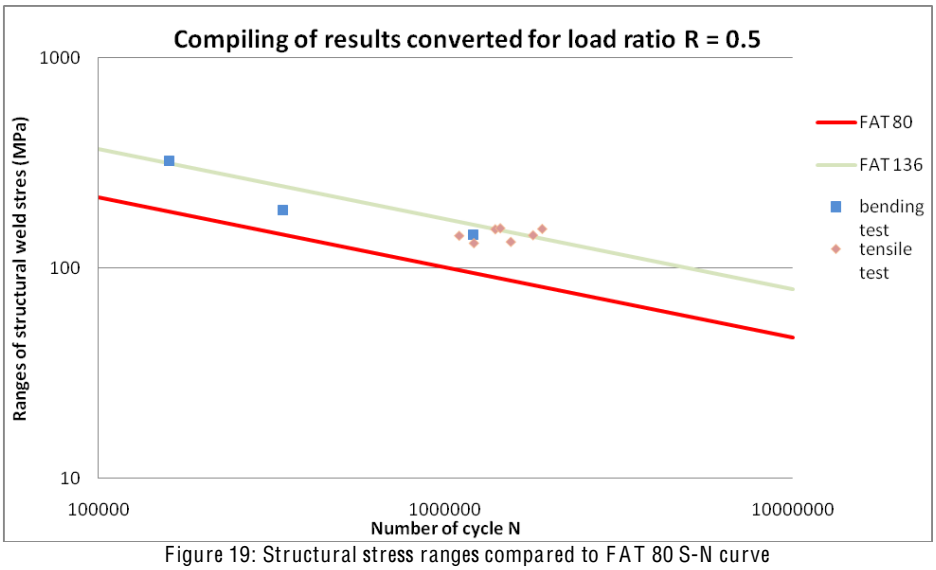

Figure 19: Structural stress ranges compared to FAT 80 S-N curve

5 WELD ROOT STRUCTURAL STRESS IMPROVEMENTS

When applying the proposed approach in order to fit test results, the limit of the proposed criteria has been reached and improvements of the method are required when the crack does not occur in the weld leg section. Fatigue tests and new structural stress calculation are presented.

5.1 Structural stress in the maximum normal stress throat section

This study is based on specimens presented in the publication XIII-2326-10 [13] by S.J.Maddox. This work involves comparative fatigue tests in tension on as-welded and weld toe peened specimens, with longitudinal non-load carrying fillet welded stiffeners as shown in figure 20. These specimens were manufactured from 30 mm thick steel

plate. UIT specimens have weld root cracks. In order to make the analysis, the author has provided additional data relative to the weld toe sizes, see figure 21, [14]. Due to the symmetry, only one half of the specimen is meshed as shown in figure 22.

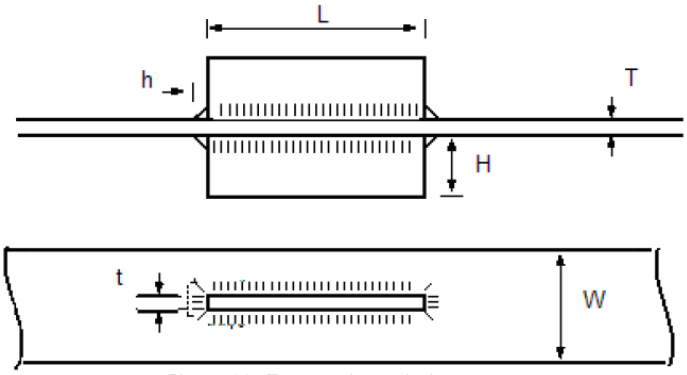

Figure 20: Test specimen design

Table 5: Specimen geometry values

L (mm)	230
W (mm)	100
T (mm)	30
t (mm)	30
H (mm)	40
h (mm)	8

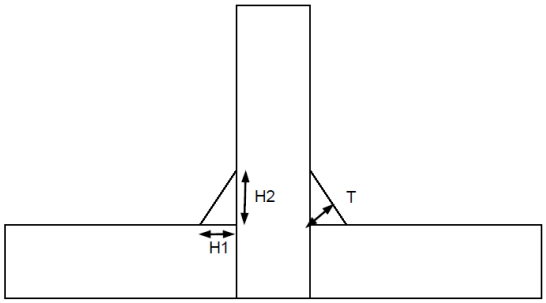

Figure 21: Seam weld design

Table 6: Weld sizes

Référence	H1 (mm)	H2 (mm)	T (mm)
UIT-1	7	14	6.26099034
UIT-2	7.5	12	6.35998728
UIT-3	8	16	7.15541753
UIT-4	10	16	8.47998304
UIT-5	7.8	15	6.92029105
UIT-6	8.7	16	7.64316167
UIT-7	8	12	6.65640235
UIT-8	8	15	7.05882353
UIT-9	8	15	7.05882353
UIT-10	8.5	17	7.60263112

H2 is the size of the weld leg in the continuation of the crack plane. It is about twice the effective throat thickness, T. When calculating the structural stress in the weld leg section, results are largely below the FAT80 S/N curve, see figure 23. In the weld leg section, shear stress is dominant and the Fricke structural stress criterion is not applicable.

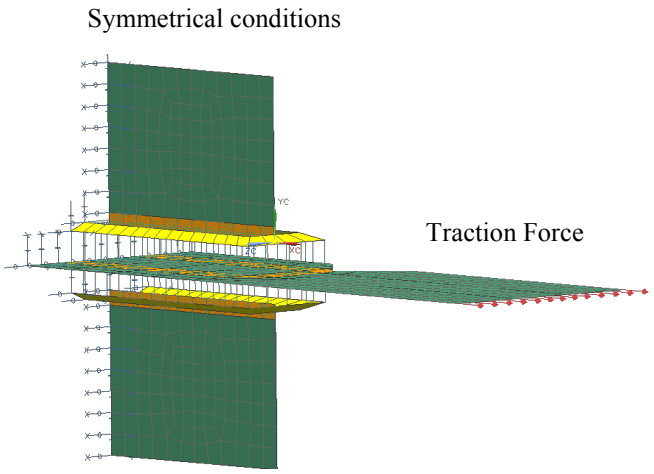

Figure 22: Boundaries conditions and application of load

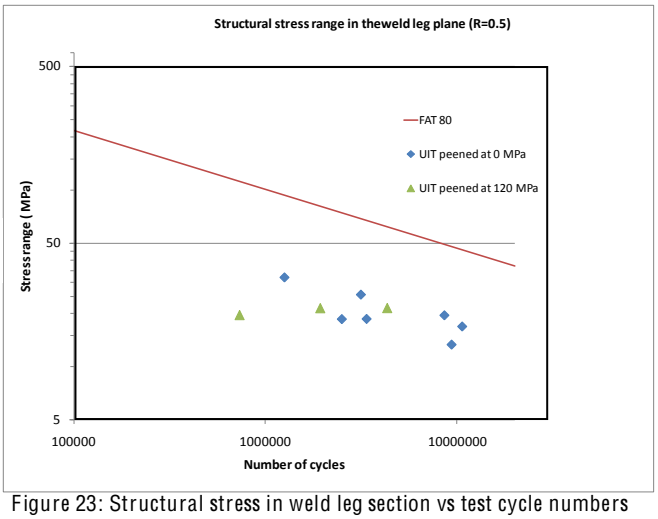

Figure 23: Structural stress in weld leg section vs test cycle numbers

The weld bead shape is unbalanced and the normal stress will increase through the weld depending on which section is considered. As we compute structural stress range in the weld leg section, the idea is to implement this calculation in other section of the weld throat. An analytical scan method of the throat has been designed to identify for which section the structural stress is the highest.

Some parameters are required to use this method (figure 24). The structural stress at the weld root is calculated for various values of theta (θ) using the following formulae.

$$\sigma_b(\theta) = \left[\left(f_y\cos\theta - f_x\sin\theta\right)\cdot\frac{\cos\theta(\tan\theta-\tan(-\beta))}{-Z_1\tan(-\beta)}\right] - \left[6\left(\frac{\cos\theta(\tan\theta-\tan(-\beta))}{-Z_1\tan(-\beta)}\right)^2\cdot\left(m_1 + \left(f_x\sin\beta + f_y\cos\beta\right)\cdot\frac{\sqrt{\left(\frac{-Z_1\tan(-\beta)}{\cos\theta(\tan\theta-\tan(-\beta))}\right)^2 + Z_1^2 - 2\left(\frac{-Z_1\tan(-\beta)}{\cos\theta(\tan\theta-\tan(-\beta))}\right)Z_1\cos\theta}}{2}\right)\right]$$

With $\beta = -\text{atan}\left(\frac{Z_2 \cos(\alpha)\tan(\alpha)}{Z_2\cos(\alpha)-Z_1}\right)$, α the seam weld angle, fx, fy and m1, extracted from the finite element model. Z1 and Z2 are the leg dimensions. For any θ value, the structural stress range associated to the section is determined. So, by scanning the angle θ, the section, where the structural stress is maximum, may be found. This weld section is designated as the maximum normal stress weld throat section.

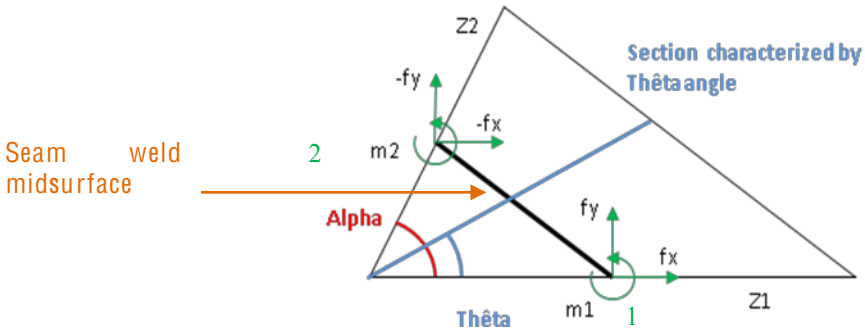

Figure 24: Scan method of the weld throat

The maximum structural stress is calculated for the Maddox specimen and the results are plotted in figure 25. Now in the critical section, the shear stress has a value lower than 20% of the structural stress and the Fricke approach may be adapted. Results show much higher stress than in the weld leg section and FAT80 may be used as a conservative design criterion.

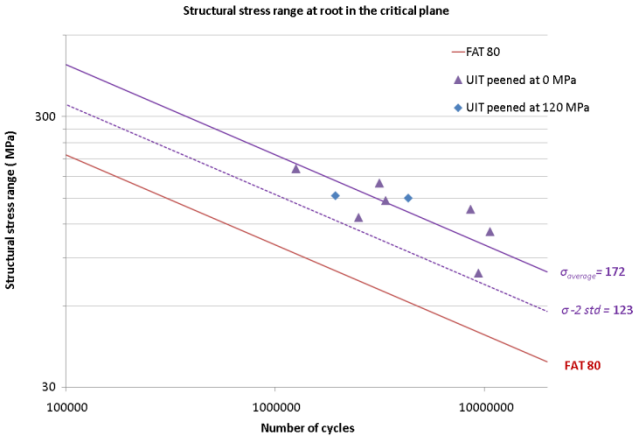

Figure 25: Critical section structural stress vs endurance cycles

5.2 Bi-axial structural stress resultant

Many fatigue tests have been performed as part of the ISCAO project. Tests involve asymmetric steel T joint assemblies with two kinds of R=0.5 loadings either tensile load or bending load. Two sizes of plate and several weld penetration parameters are investigated, see table 7.

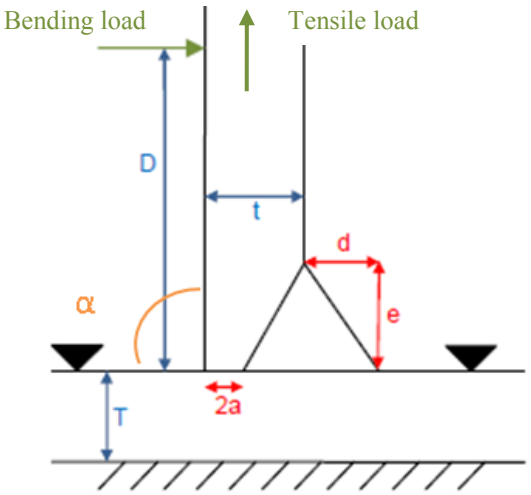

Figure 26: Steel specimen parameters

Table 7: Specimen sizes

Specimen	L1 - T	L1 - B	L3 -T	L3 - B
Load	Tensile	Bending	Tensile	Bending
Number	7	10	12	12
t (mm)	5	5	12	12
t (mm)	5	5	12	12
Width b (mm)	50	50	50	50
Deflection α (mm)	90	90	90	90
2a (mm)	3.6	3.6	1.5	1.5
d (mm)	6	6	7	7
e (mm)	5.7	5.6	15	15

For tensile tests L1-T and L3-T, the crack occurs at the weld root and propagates through the flange plate thickness. The crack angle may differ depending on the distance between the specimen supports. Structural stress is calculated at the weld root through the flange plate thickness. For bending specimens, cracks propagate through the weld throat. Structural stress is calculated in the weld leg section in the continuation of the initial crack. Only L1-T specimen results are over the FAT80 S/N curve, see figure 27.

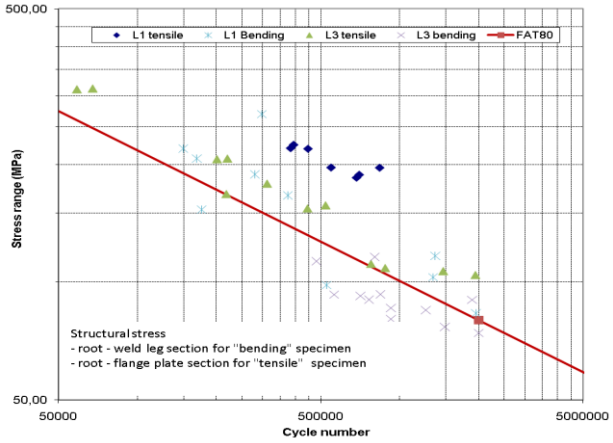

Figure 27: Flange plate and weld leg section structural stress

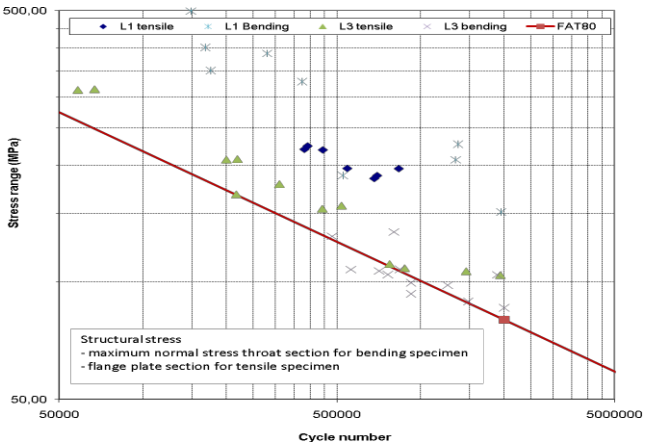

Figure 28: Flange plate and throat section maximum stress

As the L1-B specimen indicates crack propagation through the effective throat direction, the scanning method is used, the structural stress is calculated in the maximum normal stress section. The L1-B structural stresses are now over the FAT80 S/N curve as shown in figure 28. The L3 structural stress results are still not conservative. L3 specimen has a very large weld toe section, larger than the base plate thickness. For all testing configurations, the crack paths are given in the figure 29. By changing the support span of tensile specimen, the direction of crack changes. When reducing the span, the bending stress of the flange plate decreases. The three L3-T points which lie on FAT80 curve in figure 28 correspond to the narrow support span specimen. In fact, for this configuration, the normal stress in the weld throat becomes almost as high as the stress in the base plate. L3 bending specimen crack initiates at root but a little toward the flange plate when final propagation is through the weld throat. In this case, bending stress of the flange plate is as high as the normal stress in the weld leg section.

L1 tensile	L1 bending	L3 tensile High support span	L3 tensile Low support span	L3 bending
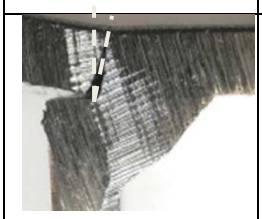	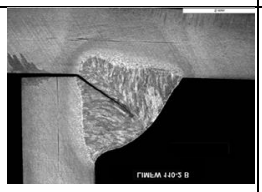		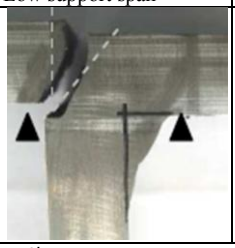	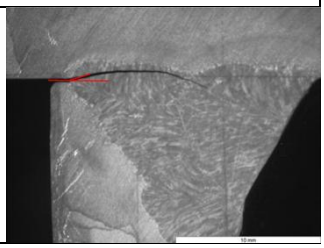

Figure 29: Crack paths

It seems that the two normal stresses, the one through the flange plate and the one through the maximum weld throat section, have to be combined in order to predict fatigue life and crack path orientation. In the weld root location, the stress tensor indicates a bi-axial stress distribution. When making a local analysis of the L3 bending test by using the fictitious 1 mm radius model, the maximum stress is reached in a nearly 45 degree direction toward the flange plate. As shown in figure 30, the maximum stress value at the weld root corresponds to the resultant of the two stress components, the stress value in a 0 degree direction normal to the weld leg section and stress value in a 90 degree direction normal to the flange plate thickness plane. Let us considerer structural stresses and the bi-axial resultant stress is defined as:

$$\sigma_S = \sqrt{\sigma_w{}^2 + \sigma_f{}^2}\ ,\quad \sigma_w \text{ normal stress in the weld and } \sigma_f \text{ normal stress in the flange plate}$$

The results are plotted in figure 31 and all data are over the FAT 80. The bi-axial resultant structural stress gives conservative results when it is compared to FAT 80 S/N curve. The resultant stress vector gives also indication of the root crack initiation direction either through the weld or through the plate.

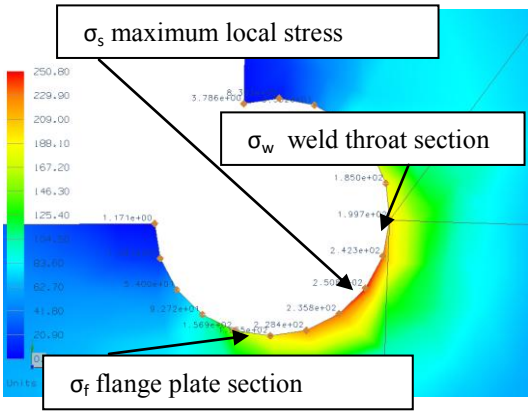

Figure 30: Local von Mises stress (MPa)

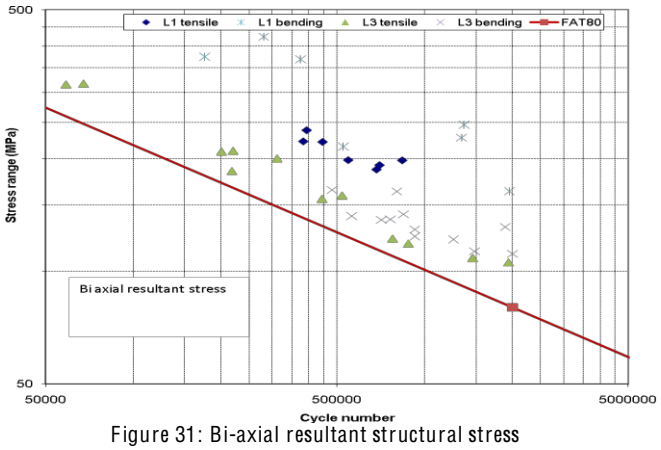

Figure 31: Bi-axial resultant structural stress

6 CAD – CAE DEVELOPMENTS

LOHR designs large structures and uses NX from SIEMENS PLM Software as CAD and CAE pre/post solutions [15]. The manual shell meshing of the weld connections is a very tedious job. A partial automation has been developed with C++ programs which use NX Open API commands and can be launched from the NX session using icons. The steps used in the CAD-CAE process are detailed with the example illustrated in figure 32. It is representative of the connection complexity. To prepare the meshing, the idea is to use the solid representation of the weld using NX weld assistant CAD tool. The selection of the two faces of the sheets to be joined provides the fillet weld seam location. The weld cross section size allocation allows the seam solid to be generated, as shown in figure 33.

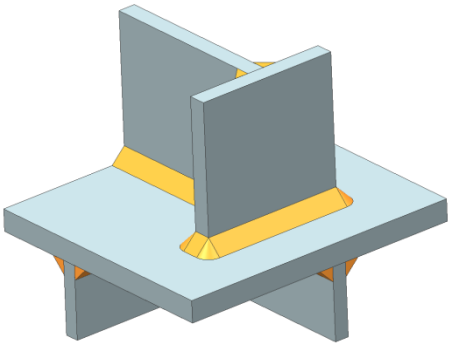

Figure 32: Weld-assembly specimen

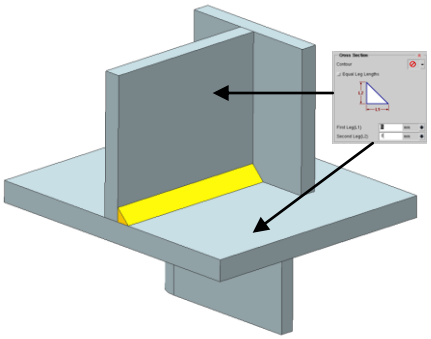

Figure 33: Weld solids

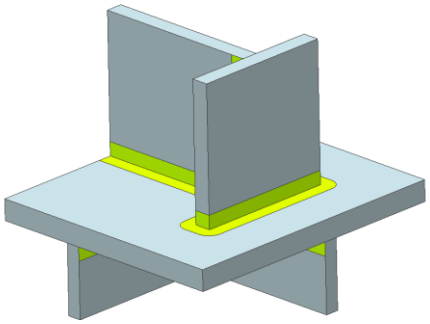

Figure 34: Weld leg imprint operation

After the CAD weld creation, the weld leg may be imprinted over the connected parts. A program makes it automatically, see figure 34. Shell meshing will be performed on the idealized mid-surfaces. The mid-surfaces are generated using CAD functionality. LOHR has developed another program which checks the mid-surface generation and transfers the weld leg imprint to the idealized faces. In order to avoid complex scar boundaries, only the envelope of the imprint is generated, see figure 35. The solid seam is also idealized to a mid-surface using the CAD tool. The connection information is reported to the idealized geometry using object attributes. When switching to the CAE NX Advanced Simulation application, the objet attributes are transferred.

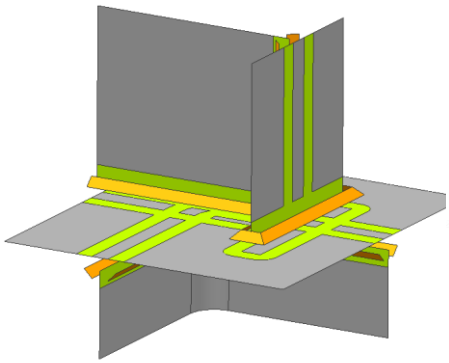

Figure 35: Imprint update to idealized geometry

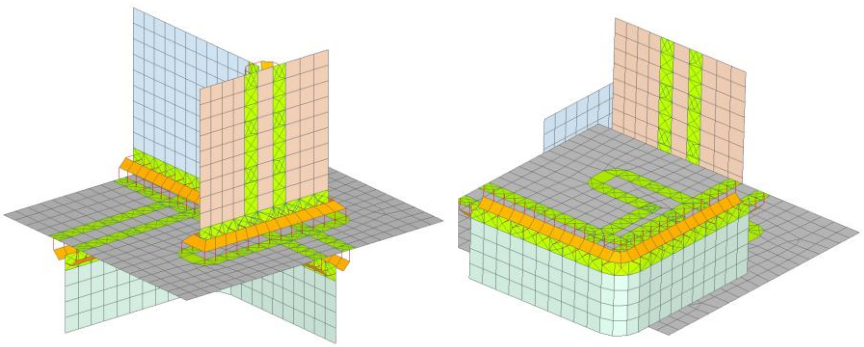

Figure 36: CAE connection operation

The shell meshing is performed manually. Once meshes are ready, the edge-to-face or edge-to-edge connections are performed automatically, see figure 36. The program activates the NX 1D connections which use the previously described mesh connection gluing technique. The global construction is based on CAD and CAE features with a robust capability for updating. The following figures (Fig 37- 38) illustrate the CAE update after modification of CAD parameters. In the present example:

1. Thicknesses are decreased
2. The weld throat sizes are decreased
3. The plate is moved
4. The faces of the plates are moved

Back in the CAE environment, the update of the meshing is performed with no manual operation

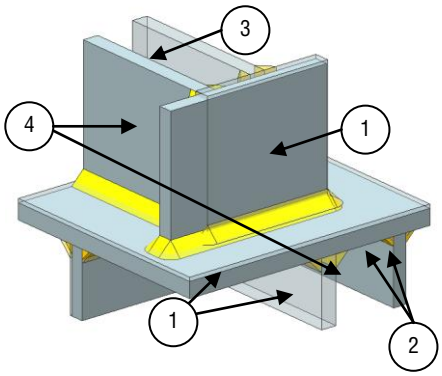

Figure 37: Geometry modification

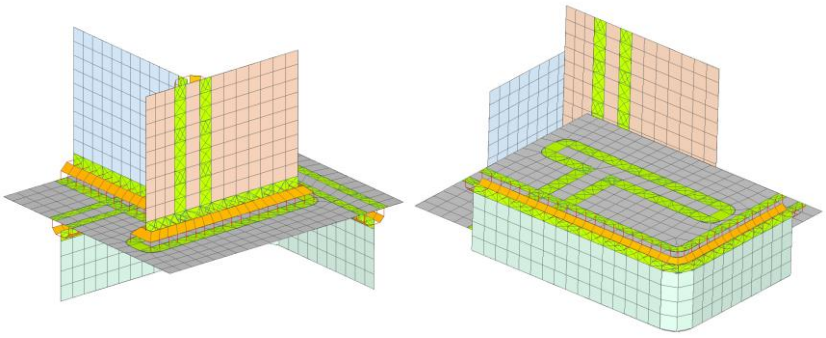

Figure 38: Update of the fem

5. INDUSTRIAL APPLICATION

Application of the method is demonstrated with the analysis of a car-carrier trailer structure, see figure 39. The FEA model is built with beam, shell and solid elements. Welds are modelized using the “seam sim” technique. The payload is introduced using concentrated masses. The kinematics joints of the upper deck and lifting devices are introduced using appropriate elastic elements. Exceptional and fatigue loads are applied using global accelerations. Static linear FEM calculation is performed using SAMCEF code [16]. The specific post analyses which compute weld static equivalent stress or fatigue stress margin are done using homemade programs which generate result file in universal format (unv file). The results display may be achieved using any FEA postview solution.

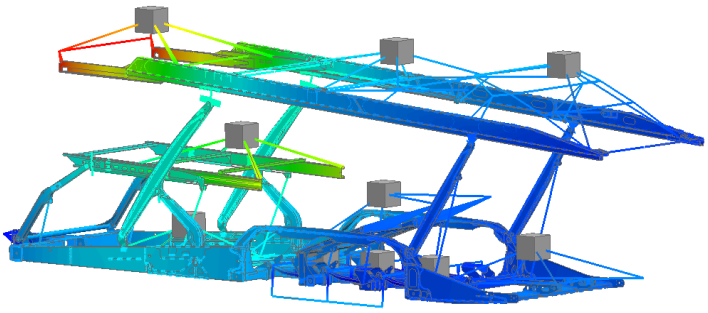

Figure 39: Entire vehicle deflection - Emergency braking

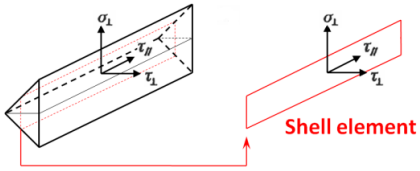

Figure 40: Equivalent stress components

For the static load cases, the weld equivalent stress σ_{eq} is calculated using formula given in §3 with the shell element stress components described in figure 40. For each seam weld, the ratio of the equivalent stress relative to the ultimate strength of the material expressed in percentage is displayed as shown in figures 41 and 42.

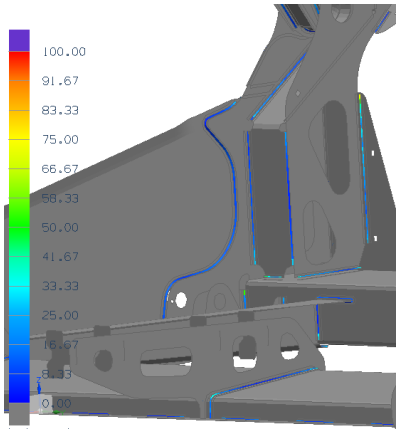

Figure 41: Static stress/ criteria ratio %

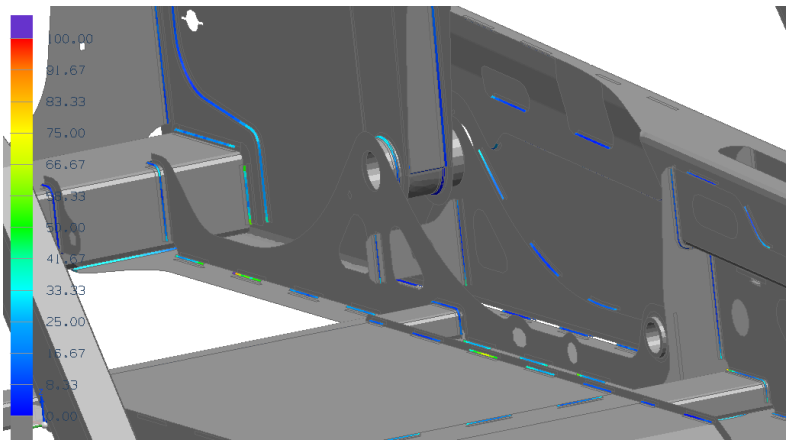

Figure 42: Static stress/ criteria ratio %

For fatigue, stress variations over the load cases are evaluated. The fatigue margin is calculated for each element by comparing the stress variation to base metal S-N curve limit. For shell elements connected to a weld leg contour, the normal stress variation in the direction perpendicular to the seam is compared to a FAT90 S-N curve. For the weld root cracking fatigue assessment, the structural stress variation in the throat section is calculated for each weld shell elements and it is compared to a FAT 80 S-N curve. All results are displayed as stress margin expressed in % and are illustrated in Figures 43 and 44.

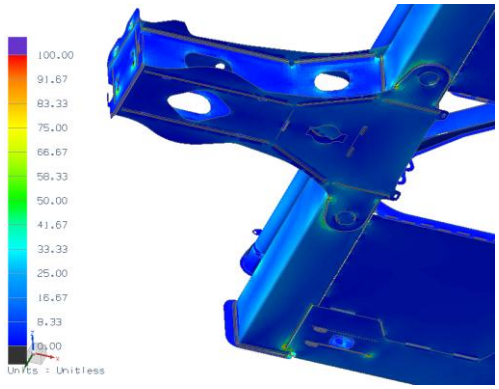

Figure 43: Fatigue stress margin expressed in %

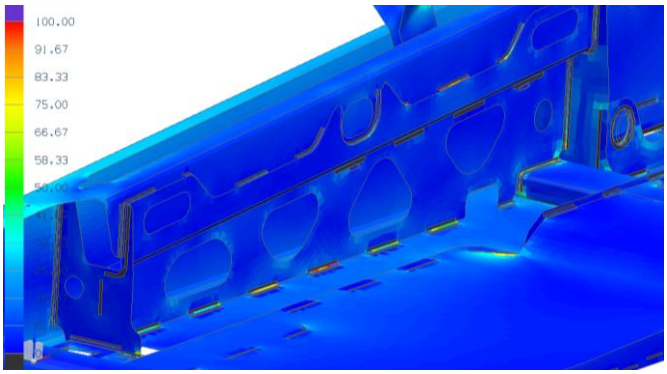

Figure 44: Fatigue stress margin expressed in %

Results display allows making the global structure fatigue assessment when considering all weld joints with the metal sheets misalignment effects. Fatigue sensitive areas are the weld joints and such detailed analyses allow making the best design for durability performance.

7 CONCLUSION

The LOHR Industrie “seam sim” project has delivered a powerful tool to make weld structural assessment with the global vehicle finite element analysis. The innovative aspect is the use of shell element and FEA gluing techniques for modelling the seam weld. This technique leads to the appropriate stiffness behaviour. Verification of the technique has been done by comparing results of the shell element model with those from a fine 3D element model. Validation has been performed by tests that have demonstrated the safe use of the FAT80 S-N curve for the weld root fatigue assessment when crack occurs in the weld leg section. Improvements of the root fatigue assessment method are defined. When weld leg sizes are unbalanced the maximum structural stress is calculated by scanning several weld throat sections. If the stress distribution at the weld root is bi-axial, the resultant of the normal structural stresses obtained in the weld throat section and in the base plate normal section is used. CAD and CAE programs, which have been developed, avoid the tedious job of manual weld meshing. The static equivalent stress and the fatigue structural stress calculations allow making the structural assessment of the weld joints. Post processing tools have been developed. They allow, in one-shot, to display either static equivalent stress or fatigue stress margin for each weld over the global structure. The fatigue design validation of the entire structure is realized through a single scalar display per element. The element S-N curve depends on the material involved for base metal or on the weld influence for either the element located at the weld toe or the weld throat element.

8 ACKNOWLEGMENTS

The major part of the work has been performed within the associative “ISCAO” project. The participants are Institut de Soudure, Siemens Industry Software and LOHR Industrie. Special thanks to Institut de Soudure for carring out the fatigue tests. Special thanks also to Geoffroy Richert and Matthieu Haab, LOHR Industrie, for the software development and testing.

9 REFERENCES

1- Turlier D, Klein P, Wilhelm A and De Azevedo M: “Seam Sim” method for seam weld structural assessment using shell element FEA model. NAFEMS UK conference June 21010, NAFEMS Benchmark April 2010 and Institut de Soudure Infos Membres N°2 2010.
2- Turlier D, Klein P and Bérard F (2010): “Seam Sim” method for seam weld structural assessment within a structure FEA. Proc. Int. Conf. IIW2010 Istanbul (Turkey). AWST, 651-658
3- Eurocode 3 (1992) / P 22-311-M “Design of steel structures” and National Application Document –Part 1-1: General rules and rules for buildings – Annex M: Alternative method for fillet welds
4- Niemi E, Fricke W, Maddox S J (2006): Fatigue analysis of welded components Designer’s guide to the structural hot spot stress approach. IIW-1430-00, Woodhead Publishing.
5- Fricke W, Kahl A, Paetzold H (2006): Fatigue assessment of root cracking of fillet welds subject to throat bending using the structural stress approach, Doc IIW-1737-06.
6- Fricke W (2011): “IIW Guideline for the Assessment of Weld Root Fatigue” IIW-Doc. XIII-2380r1-11/XV-1383r1-11
7- Hobbacher A (2009): Recommendations for Fatigue Design of Welded Joints and Components, IIW doc.1823-07, Welding Research Council Bulletin 520, New York.
8-FKM Guideline (2003): Analytical strength assessment
9-C. M. Sonsino (2008): Suggested allowable equivalent stresses for fatigue design of welded joints according to the notch stress concept with the reference radii rref=1.00 and 0.05 mm, IIW-Doc XIII-2216-08 / XV 1285-08.
10- Sonsino C M and Wiebesiek J (2007): Assessment of multiaxial spectrum loading of welded steel and aluminium joints by modified equivalent stress. IIW-Doc. XIII-2158r1-07/XV-1250r1-07
11- Institut de Soudure RT-45058 : IS rapport technique
12- Institut de Soudure RT-31922 : IS rapport technique
13- Maddox S J, Doré M J and Smith S.D (2010): Investigation of Ultrasonic Peening for Upgrading a Welded Steel Structure, Doc IIW-XIII-2326-10
14- P.Y. Lahorgue (2011): Weld root fatigue assessment using structural stress approach of the IIW XIII-2326-10 S.J Maddox specimens, LOHR D00001944A.
15- SIEMENS PLM Software NX7.5 Advanced simulation help library
16- SAMTECH, Samcef User Manual V14.1